Monatsh Chem 139, 1143–1149 (2008)
DOI 10.1007/s00706-008-0914-4
Printed in The Netherlands

Monatshefte für Chemie
Chemical Monthly

Structure and properties of $Ce_3Pd_3Bi_4$, CePdBi, and $CePd_2Zn_3$

Wilfried Hermes[1], Stefan Linsinger[1], Ratikanta Mishra[1,2], Rainer Pöttgen[1]

[1] Institut für Anorganische und Analytische Chemie and NRW Graduate School of Chemistry, Westfälische Wilhelms-Universität Münster, Münster, Germany
[2] Bhabha Atomic Research Centre, Chemistry Division, Trombay, Mumbai, India

Received 11 February 2008; Accepted 22 February 2008; Published online 15 May 2008

Abstract The intermetallic cerium compounds $Ce_3Pd_3Bi_4$, CePdBi, and $CePd_2Zn_3$ were synthesized from the elements in sealed tantalum ampoules in an induction furnace. The compounds were characterized by X-ray powder and single crystal diffraction: $CeCo_3B_2$ type (ordered version of $CaCu_5$), $P6/mmm$, $a = 538.4(4)$, $c = 427.7(4)$ pm, $wR2 = 0.0540$, 115 F^2 values, 9 variables for $CePd_2Zn_3$ and $Y_3Au_3Sb_4$ type, $I\bar{4}3d$, $a = 1005.2(2)$ pm, $wR2 = 0.0402$, 264 F^2 values, 9 variables for $Ce_3Pd_3Bi_4$, and MgAgAs type, $a = 681.8(1)$ pm for CePdBi. The bismuthide structures are build up from three-dimensional networks of corner-sharing $PdBi_4$ tetrahedra with Pd–Bi distances of 281 ($Ce_3Pd_3Bi_4$) and 296 pm (CePdBi), respectively. The cerium atoms are located in larger voids of coordination number 12 ($Ce_3Pd_3Bi_4$) and 10 (CePdBi). In $CePd_2Zn_3$ the cerium atoms fill larger channels within the three-dimensional $[Pd_2Zn_3]$ network with 18 (6 Pd + 12 Zn) nearest neighbors. The three compounds contain stable trivalent cerium with experimental magnetic moments of $\mu_{eff} = 2.70(2)$, 2.48(1), and 2.49(1) μ_B/Ce atom for $CePd_2Zn_3$, $Ce_3Pd_3Bi_4$, and CePdBi, respectively. Susceptibility and specific heat data gave no hint for magnetic ordering down to 2.1 K.

Correspondence: Rainer Pöttgen, Institut für Anorganische und Analytische Chemie and NRW Graduate School of Chemistry, Westfälische Wilhelms-Universität Münster, Corrensstrasse 30, 48149 Münster, Germany. E-mail: pottgen@uni-muenster.de

Keywords Cerium compounds; Crystal chemistry; Magnetic properties; X-Ray structure.

Introduction

The equiatomic Ce*TX* compounds (*T* = late transition metal; *X* = element of the 3rd or 4th main group) have intensively been investigated in recent years with respect to their hydrogenation behavior (overviews are given in Refs. [1–4]), since the hydrogenation drastically changes the magnetic ground state of cerium. To give an example, hydrogen insertion leads to an interesting transition from an intermediate valence state in CeNiIn to a ferromagnetic behaviour in $CeNiInH_{1.8}$ [5], or an increase of the *Néel* temperature (1.65 K → 3.0 K) in the sequence CePdIn (*Kondo* antiferromagnet) → $CePdInH_{1.0}$ [6]. We have recently extended these investigations towards the Ce*TX* compounds with respect to the group V systems. Hydrogenation of the *Kondo* semiconductor CeRhSb induces antiferromagnetic behaviour in the new hydride $CeRhSbH_{0.2}$ [7].

In continuation of these systematic investigations we were interested in the hydrogenation behavior of further Ce*TX* systems and we are currently testing the Ce*T*Bi and Ce*T*Zn compounds. In the bismuth and zinc containing systems, so far the equiatomic compounds Ce*T*Bi (*T* = Rh, Pd, Pt) [8–10] and Ce*T*Zn (*T* = Ni, Cu, Rh, Pd, Ag, Pt, Au) [11–16] have been reported. During our synthetic studies

we obtained a pure sample of CePdBi for physical property investigations. In the first steps, new compounds $Ce_3Pd_3Bi_4$ and $CePd_2Zn_3$ were obtained as side products. Herein we report on the phase pure synthesis, crystal growth, and the magnetic properties of these intermetallic compounds.

Results and discussion

Structure refinements

Careful analysis of the diffractometer data sets revealed high *Laue* symmetry for both crystals. The data sets were compatible with space groups $P6/mmm$ for $CePd_2Zn_3$ and $I\bar{4}3d$ for $Ce_3Pd_3Bi_4$. The isotypism with the $CaCu_5$ [17] ($CeCo_3B_2$ [18]) and $Y_3Au_3Sb_4$ [19] type was already evident from the powder patterns. The atomic parameters of $CaCu_5$ and $Y_3Au_3Sb_4$ were taken as starting values and the two structures were refined using SHELXL-97 [20] (full-matrix least-squares on F^2) with anisotropic atomic displacement parameters for all atoms. Refinement of the correct absolute structure for $Ce_3Pd_3Bi_4$ was ensured through calculation of the *Flack* parameter [21, 22]. As a check for the correct composition, the occupancy parameters of all sites were refined in separate series of least-squares cycles. All sites were fully occupied (with the coloring Co $\Longleftrightarrow$ Zn and B $\Longleftrightarrow$ Pd for $CePd_2Zn_3$) within two standard deviations and in the final cycles the ideal occupancy parameters were assumed again. The final difference *Fourier* syntheses were flat (Table 1). The positional parameters and interatomic distances of the two refinements are listed in Tables 2 and 3. Further details may be obtained from Fachinformationszentrum Karlsruhe, D-76344 Eggenstein-Leopoldshafen (Germany), by quoting the Registry Nos. CSD-419163 ($CePd_2Zn_3$) and CSD-419162 ($Ce_3Pd_3Bi_4$).

Crystal chemistry

New intermetallic compounds $CePd_2Zn_3$ and $Ce_3Pd_3Bi_4$ have been synthesized and structurally characterized on the basis of single crystal diffractometer data. Similar to a large variety of rare earth metal

Table 1 Crystal data and structure refinement for $Ce_3Pd_3Bi_4$ and $CePd_2Zn_3$

Empirical formula	$Ce_3Pd_3Bi_4$	$CePd_2Zn_3$
Molar mass/g mol^{-1}	1575.48	549.03
Space group; Z	$I\bar{4}3d$; 4	$P6/mmm$; 1
Structure type	$Y_3Au_3Sb_4$	$CaCu_5$
Pearson symbol	cI40	hP6
Unit cell dimensions/pm	$a = 1005.2(2)$	$a = 538.4(4)$
(*Guinier* powder data)		$c = 427.7(4)$
Unit cell volume/nm^{-3}	$V = 1.0157$	$V = 0.1074$
Calculated density/g cm^{-3}	10.30	8.49
Crystal size/μm^3	$30 \times 40 \times 70$	$20 \times 40 \times 60$
Transm. ratio (max/min)	7.09	1.39
Absorption coefficient/mm^{-1}	87.3	34.8
$F(000)$	2576	240
θ Range/°	4–31	4–40
Range in *hkl*	± 13; $-13/14$; ± 14	$-7/8$; $-9/7$; ± 6
Total no. reflections	4645	1345
Independent reflections	264 ($R_{int} = 0.1366$)	115 ($R_{int} = 0.0429$)
Reflections with $I > 2\sigma(I)$	210 ($R_\sigma = 0.0825$)	106 ($R_\sigma = 0.0157$)
Data/parameters	264/9	115/9
Goodness-of-fit on F^2	0.726	1.286
Final R indices [$I > 2\sigma(I)$]	$R1 = 0.0232$	$R1 = 0.0209$
	$wR2 = 0.0381$	$wR2 = 0.0530$
R indices (all data)	$R1 = 0.0415$	$R1 = 0.0232$
	$wR2 = 0.0402$	$wR2 = 0.0540$
Extinction coefficient	0.00182(8)	0.036(5)
Flack parameter	$-0.04(2)$	–
Largest diff. peak and hole/e Å^{-3}	$1.89/-1.81$	$1.54/-2.36$

Table 2 Atomic coordinates and anisotropic displacement parameters (pm^2) for $Ce_3Pd_3Bi_4$ and $CePd_2Zn_3$. U_{eq} is defined as one third of the trace of the orthogonalized U_{ij} tensor. The anisotropic displacement factor exponent takes the form $-2\pi^2[(ha^*)^2U_{11}+\ldots+2kha^*b^*U_{12}]$

Atom	*Wyckoff* position	*x*	*y*	*z*	U_{11}	U_{22}	U_{33}	$U_{13}=U_{23}$	U_{12}	U_{eq}
$Ce_3Pd_3Bi_4$										
Ce	12*b*	5/8	0	3/4	87(7)	63(4)	U_{22}	0	0	71(3)
Pd	12*a*	1/8	0	3/4	75(9)	100(6)	U_{22}	0	0	92(4)
Bi	16*c*	0.91607(5)	*x*	*x*	74(2)	U_{11}	U_{11}	14(2)	U_{13}	74(2)
$CePd_2Zn_3$										
Ce	1*a*	0	0	0	67(2)	U_{11}	87(4)	0	34(1)	74(2)
Pd	2*c*	1/3	2/3	0	108(2)	U_{11}	70(4)	0	54(1)	95(2)
Zn	3*g*	1/2	0	1/2	132(4)	75(4)	77(4)	0	37(2)	101(3)

Table 3 Interatomic distances pm, calculated with the powder lattice parameters in $Ce_3Pd_3Bi_4$ and $CePd_2Zn_3$. Standard deviations are all equal or less than 0.2 pm. All distances of the first coordination spheres are listed

$Ce_3Pd_3Bi_4$				$CePd_2Zn_3$			
Ce	4	Pd	307.8	Ce	6	Pd	310.8
	4	Bi	347.3		12	Zn	343.8
	4	Bi	348.6	Pd	6	Zn	264.4
Pd	4	Bi	281.2		3	Pd	310.9
	4	Ce	307.8		3	Ce	310.9
Bi	3	Pd	281.2	Zn	4	Pd	264.4
	3	Ce	347.3		4	Zn	269.2
	3	Ce	348.6		4	Ce	343.8
	3	Bi	374.1				

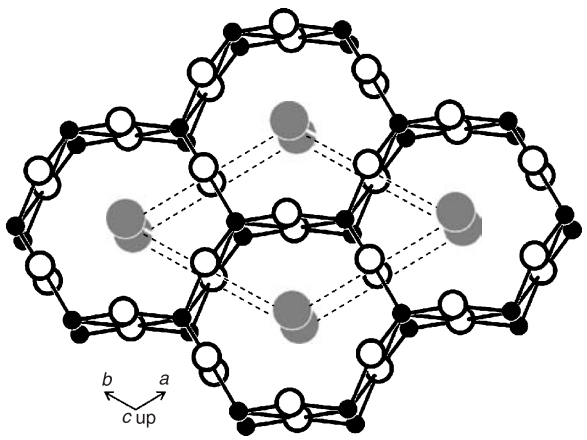

Fig. 1 View of the $CePd_2Zn_3$ structure approximately along the *c* axis. Cerium, palladium, and zinc atoms are drawn as medium grey, black filled, and open circles. The three-dimensional $[Pd_2Zn_3]$ network is emphasized

based compounds [23, 24], $CePd_2Zn_3$ (Fig. 1) crystallizes with an ordered version of the well known hexagonal $CaCu_5$ type structure [17], similar to $CeCo_3B_2$ [21]. The palladium and zinc atoms occupy the *Wyckoff* sites 2*c* and 3*g* in an ordered manner. Together, the palladium and zinc atoms build up a three-dimensional $[Pd_2Zn_3]$ network (Fig. 1), which leaves larger hexagonal channels for the cerium atoms. Within the $[Pd_2Zn_3]$ network, each palladium atom has six nearest zinc neighbors at 264 pm in trigonal prismatic coordination. Similar coordination occurs for the Pd1 atoms in α-CePdZn (268 pm) [25]. These Pd–Zn distances are only slightly longer than the sum of the covalent radii of 253 pm [26]. The cerium atoms bind to the $[Pd_2Zn_3]$ network through Ce–Pd contacts at a Ce–Pd distance of 311 pm. The Zn–Zn distances of 269 pm (triangular edges of the trigonal prisms) are close to the shorter distances in *hcp* zinc (6×266 and 6×291 pm) [27]. We can therefore expect substantial Pd–Zn and Zn–Zn bonding in the $[Pd_2Zn_3]$ network.

Also the binary boarder phases $CePd_5$ ($a=537.2$, $c=417.8$ pm) [28] and $CeZn_5$ ($a=541.63(5)$, $c=426.47(5)$ pm) [29] with $CaCu_5$ type structure have been reported. The ordered compound $CePd_2Zn_3$ fits in between these data. Similar transition metal ordering has recently been observed for $CaNi_2Zn_3$ [30], however, due to differences in size, an isomorphic symmetry reduction of index 3 (i3) leads to superstructure formation and thus small distortions in the structure. No hints for a cell enlargement have been observed for $CePd_2Zn_3$ reported herein. For further crystal chemical details on the family of $CaCu_5$ related intermetallics we refer to the TYPIX compilation [24, and references therein].

$Y_3Au_3Sb_4$ type [19] $Ce_3Pd_3Bi_4$ is a new compound in the Ce–Pd–Bi system [10]. So far only CePdBi [8] (*vide ultra*) and $Ce_8Pd_{24}Bi$ [31] have been reported. The cubic $Ce_3Pd_3Bi_4$ structure con-

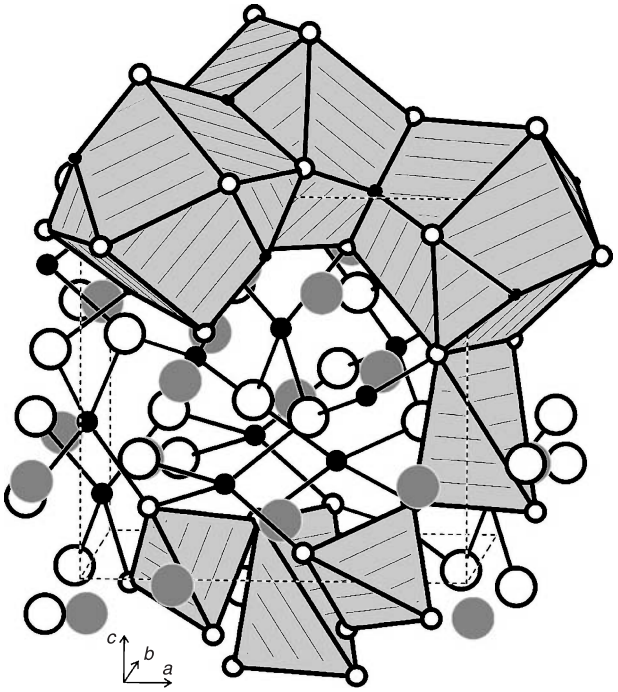

Fig. 2 The crystal structure of $Ce_3Pd_3Bi_4$. Cerium, palladium, and bismuth atoms are drawn as medium grey, black filled, and open circles, respectively. The $PdBi_4$ tetrahedra and the CN12 coordination polyhedra of the cerium atoms are emphasized. For details see text

tains two striking structural motifs, *i.e.* slightly distorted, corner-sharing $PdBi_4$ tetrahedra and coordination number (CN) 12 polyhedra (4Pd + 8Bi) around the cerium atoms. The Pd–Bi distances of 281 pm match with the sum of the covalent radii of 280 pm [26] and these are most likely the strongest bonding interactions in $Ce_3Pd_3Bi_4$. The cerium atoms are embedded within the network of condensed tetrahedra (Fig. 2). As emphasized in the upper part of that figure, the CN12 polyhedra of the cerium atoms are condensed *via* common square faces, leading to a dense packing. These CN12 polyhedra share common edges with the $PdBi_4$ tetrahedra. Similar to $CePd_2Zn_3$, also in $Ce_3Pd_3Bi_4$ the cerium atoms have four palladium atoms as closest neighbours. This would have been expected from the course of the electronegativities.

Equiatomic CePdBi [8] has only been obtained in polycrystalline form. Since all atoms in this MgAgAs type [32] compound are on special positions, the interatomic distances can readily be calculated from the lattice parameter (681.8(1) pm). The cerium and bismuth atoms build up a rocksalt like substructure in which half of the tetrahedral voids

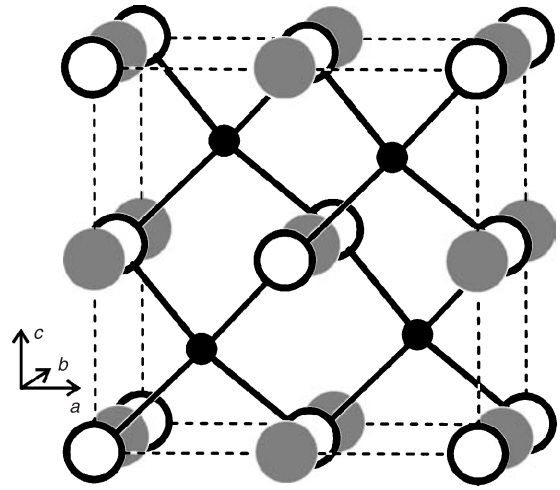

Fig. 3 The crystal structure of CePdBi. Cerium, palladium, and bismuth atoms are drawn as medium grey, black filled, and open circles. The corner-sharing $PdBi_4$ tetrahedra are emphasized

are filled with palladium (Fig. 3). This way the palladium atoms have a tetrahedral bismuth coordination at Pd–Bi distances of 296 pm, somehow longer than in $Ce_3Pd_3Bi_4$. On the other hand, the Ce–Pd distance of 296 is by 12 pm shorter than in $Ce_3Pd_3Bi_4$. The crystal chemistry of MgAgAs type intermetallic compounds has repeatedly been discussed in literature. For further details we refer to the TYPIX compilation [24, and references therein] and a recent work on equiatomic *RET*Bi (*RE* = rare earth element) bismuthides [33].

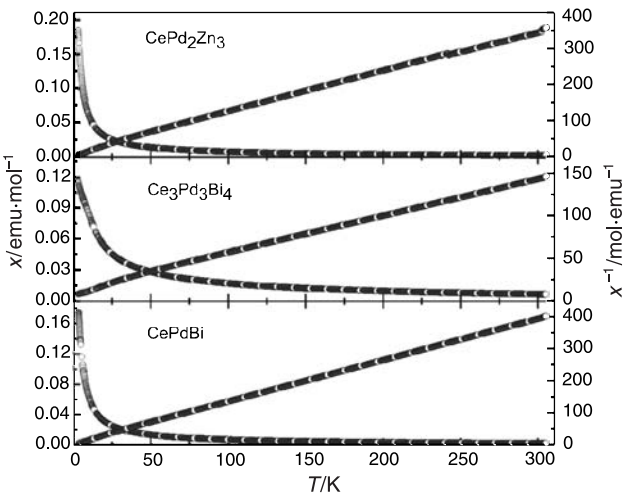

Fig. 4 Temperature dependence of the magnetic dc susceptibility (χ and χ^{-1}) of $CePd_2Zn_3$, $Ce_3Pd_3Bi_4$, and CePdBi measured at a magnetic flux density of 1 T

Magnetic properties

The temperature dependences of the magnetic ($\chi = M/H$) and the inverse magnetic susceptibility of $CePd_2Zn_3$, $Ce_3Pd_3Bi_4$, and CePdBi are displayed in Fig. 4, measured while warming in a dc field of 10 kOe after zero field cooling each sample to lowest temperature. For all samples studied here, χ increases with decreasing temperature. Down to 3.1 K, the magnetic data give no hint for magnetic ordering in all three samples.

The three samples show *Curie-Weiss* behavior (Fig. 4). Fitting of the experimental data in the temperature region 100–300 K revealed an effective magnetic moment of $\mu_{eff} = 2.70(2)$ μ_B/Ce atom and a paramagnetic *Curie* temperature $\theta_P = -19.0(2)$ K for $CePd_2Zn_3$, $\mu_{eff} = 2.48(1)$ μ_B/Ce atom, and $\theta_P = -32.7(2)$ K for $Ce_3Pd_3Bi_4$ and $\mu_{eff} = 2.49(1)$ μ_B/Ce atom and $\theta_P = -5.8(2)$ K for CePdBi. These values are close to the free ion value of 2.54 μ_B for Ce^{3+}, thus indicating purely trivalent cerium in all samples. The negative sign of θ_P indicates that the magnetic interaction is of an antiferromagnetic type in these compounds. The deviations of $1/\chi$ *vs.* T at low temperatures are most likely due to splitting of the $J = 5/2$ ground state of Ce^{3+} and the beginning of short-range magnetic fluctuations, as frequently observed in related cerium intermetallics, *e.g.* CeAuGe [34] and $CeRhSn_2$ [35].

In Fig. 5 we present the magnetization data for $CePd_2Zn_3$ and $Ce_3Pd_3Bi_4$ measured at 5, 10, and 15 K. $CePd_2Zn_3$ shows at 5 K a tendency for saturation in high fields. At 10 and 15 K $CePd_2Zn_3$ shows

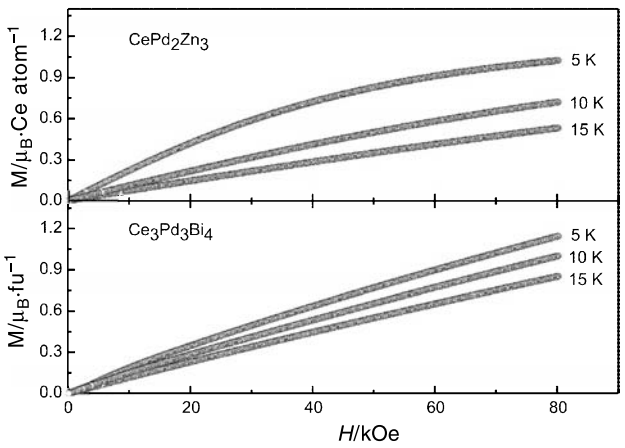

Fig. 5 The M(H) curves for $CePd_2Zn_3$ and $Ce_3Pd_3Bi_4$ measured at 5, 10, and 15 K

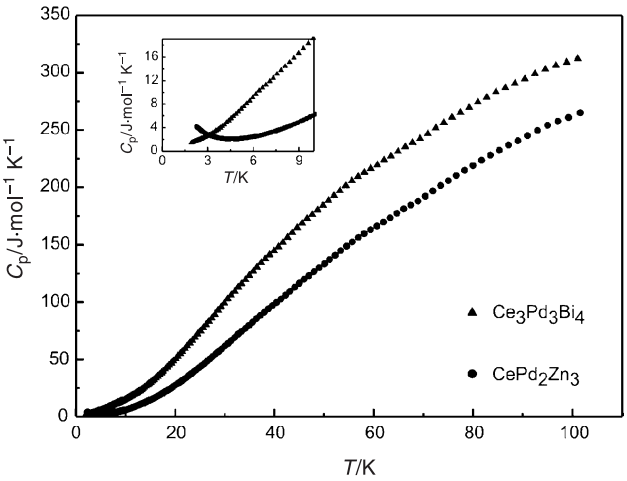

Fig. 6 The specific heat (C_P) data for $CePd_2Zn_3$ and $Ce_3Pd_3Bi_4$ measured in zero field

almost linear $M(H)$ behavior in agreement with the paramagnetic state of the sample. The magnetization curves for $Ce_3Pd_3Bi_4$ are almost linear for all measured temperatures as expected for a paramagnetic material. It may be noted here that, for both compounds, the maximum moment observed at 80 kOe and 5 K does not reach the expected moment value of 2.14 μ_B/Ce atom (according to $g \times J$). The values for $CePd_2Zn_3$ and $Ce_3Pd_3Bi_4$ are 1.00(2) and 0.38(2) μ_B/Ce atom, respectively. The decrease in saturation moment can be attributed to crystal field effects (see also the deviation of $\chi(T)$ from the *Curie-Weiss* fit), and has been observed for many other cerium intermetallics [36, 37, and references therein]. The magnetic and specific heat data (Fig. 6) give no hint for magnetic ordering down to 2.1 K.

Experimental

Synthesis

Starting materials for the preparation of CePdBi, $Ce_3Pd_3Bi_4$, and $CePd_2Zn_3$ were ingots of cerium (Johnson Matthey or Kelpin), palladium powder (Degussa-Hüls, 200 mesh), zinc granules (Merck), and bismuth granules (Chempur) all with stated purities better than 99.9%. The cerium ingots were cut into smaller pieces and arc-melted [38] into small buttons under an argon atmosphere. The argon was purified before with molecular sieves, silica gel, and titanium sponge (900 K). Subsequently, the cerium buttons, the palladium powder, and pieces of the zinc granules or bismuth (1:2:3, 1:1:1, or 3:3:4 atomic ratio) were sealed in tantalum tubes under an argon pressure of *ca.* 700 mbar. The tube was placed in a water-cooled sample chamber of an induction furnace (Hüttinger Elektronik, Freiburg, and type TIG 1.5/300) under flowing

argon [39] and was annealed at 1400 K for about 5 min followed by slow cooling to 970 K for $CePd_2Zn_3$ and to 870 K for $Ce_3Pd_3Bi_4$. Finally the samples were kept at that temperature for another 4 h, followed by quenching. In the case of CePdBi, the tube was annealed for about 3 h at 870 K followed by fast heating to 1400 K and kept at that temperature for 5 min. The power supply was then switched off and the sample was annealed again for another two times at 1400 K (5 min for each annealing sequence). Finally the sample was annealed at 870 K for 3 h and cooled to room temperature within 5 min. The temperature was controlled through a Sensor Therm Methis MS09 pyrometer with an accuracy of ± 30 K. The samples could easily be separated from the crucibles. No reactions with the container material (tantalum) were observed. $CePd_2Zn_3$ is stable in air over weeks, while $Ce_3Pd_3Bi_4$ and CePdBi were kept in argon-filled *Schlenk* tubes because they are slightly sensitive to moist air. Single crystals exhibit metallic lustre while ground powders are grey.

Scanning electron microscopy

Semiquantitative EDX analyses on all bulk samples and single crystals were carried out by use of a Leica 420i scanning electron microscope with CeO_2, palladium, bismuth, and zinc as standards. The crystals mounted on a quartz fibre were first coated with a thin carbon film to ensure conductivity. The polycrystalline samples were embedded in a methyl metacrylate matrix and polished with different diamond and SiO_2 emulsions. No impurity elements heavier than sodium (detection limit of the instrument) were detected. The experimentally determined compositions were very close to the ideal ones. The EDX analyses gave no hints of homogeneity ranges.

X-Ray data collection

The polycrystalline samples were studied through *Guinier* powder patterns (imaging plate technique, Fujifilm BAS-1800) using Cu$K\alpha_1$ radiation and α-quartz ($a = 491.30$ and $c = 540.46$ pm) as an internal standard. The lattice parameters (Table 1) were obtained from least-squares fits of the powder data. To ensure proper indexing, the experimental patterns were compared to calculated ones [19] taking the atomic positions from the structure refinements (Table 2). The powder and single crystal lattice parameters agreed well.

Small single crystals of $Ce_3Pd_3Bi_4$ and $CePd_2Zn_3$ (CePdBi was obtained only in polycrystalline form) were selected from the annealed samples and first investigated via *Laue* photographs on a *Buerger* camera (white Mo radiation), equipped with the same Fujifilm, BAS-1800 imaging plate technique, in order to check the quality for intensity data collection. Intensity data of the $CePd_2Zn_3$ crystal were collected at room temperature by use of a four-circle diffractometer (CAD4) with graphite monochromatized Mo Kα radiation and a scintillation counter with pulse height discrimination. The scans were taken in the $\omega/2\theta$ mode and an empirical absorption correction was applied on the basis of psi-scan data, accompanied by a spherical absorption correction. The $Ce_3Pd_3Bi_4$ crystal was measured on a *Stoe* IPDS II diffractometer (graphite monochromatized Mo Kα radiation; oscillation mode; 90 mm crystal-detector distance; 0–180° phi range; 1° phi increment; 5 min irradiation time) and a numerical absorption correction was applied to this data set. All relevant details concerning the data collections and evaluations are listed in Table 1.

Physical property measurements

$CePd_2Zn_3$, CePdBi, and $Ce_3Pd_3Bi_4$ were packed in kapton foil and attached to the sample holder rod of a VSM for measuring the magnetic properties in a Quantum Design Physical-Property-Measurement-System in the temperature range 3.1–305 K with magnetic flux densities up to 80 kOe. For heat capacity (C_P) measurements (2.1–100 K) the samples were glued to the platform of a pre-calibrated heat capacity puck using *Apiezion N grease*.

Acknowledgements

This work was financially supported by the Deutsche Forschungsgemeinschaft. *W. Hermes* is indebted to the Fonds der Chemischen Industrie for a PhD stipend. *R. Mishra* thanks the *Alexander-von-Humboldt* Foundation for a research stipend.

References

1. Chevalier B, Bobet J-L, Pasturel M, Gaudin E, Etourneau J (2003) J Alloys Compd 356–357:147
2. Chevalier B, Pasturel M, Bobet J-L, Decourt R, Etourneau J, Isnard O, Sanchez Marcos J, Rodriguez Fernandez J (2004) J Alloys Compd 383:4
3. Chevalier B, Pasturel M, Bobet J-L, Isnard O (2005) Solid State Commun 134:529
4. Bobet J-L, Pasturel M, Chevalier B (2006) Intermetallics 14:544
5. Chevalier B, Kahn ML, Bobet J-L, Pasturel M, Etourneau J (2002) J Phys Condens Matter 14:L365
6. Chevalier B, Wattiaux A, Bobet J-L (2006) J Phys: Condens Matter 18:1743
7. Chevalier B, Decourt R, Heying B, Schappacher FM, Rodewald UCh, Hoffmann R-D, Pöttgen R, Eger R, Simon A (2007) Chem Mater 19:28
8. Marazza R, Rossi D, Ferro R (1980) Gazz Chim Ital 110:357
9. Yoshii S, Tazawa D, Kasaya M (1997) Physica B 230–232:380
10. Gschneidner Jr KA, Bünzli J-CG, Pecharsky VK (2006) Mar A, Bismuthides. In: Handbook on the Physics and Chemistry of Rare Earths, vol 36. Elsevier, Amsterdam, Chapter 227, p 1
11. Iandelli A (1992) J Alloys Compd 182:87
12. Morin P, Gignoux D, Voiron J, Murani AP (1992) Physica B 180 & 181:173
13. Fornasini ML, Iandelli A, Merlo F, Pani M (2000) Intermetallics 8:239
14. Mishra R, Hermes W, Pöttgen R (2007) Z Naturforsch 62b:1581

15. Hermes W, Mishra R, Rodewald UCh, Pöttgen R (2008) Z Naturforsch 63b:537
16. Hermes W, Al Alam AF, Matar SF, Pöttgen R (2008) Solid State Sci, in press
17. Haucke W (1940) Z Anorg Allg Chem 244:17
18. Kuzma YuB, Krypyakevich PI, Bilonizhko NS (1969) Dopov Akad Nauk Ukr RSR Ser A:939
19. Dwight AE (1977) Acta Crystallogr B 33:1579
20. Sheldrick GM (1997) SHELXL-97, Program for Crystal Structure Refinement, University of Göttingen
21. Flack HD, Bernadinelli G (1999) Acta Crystallogr 55A:908
22. Flack HD, Bernadinelli G (2000) J Appl Crystallogr 33:1143
23. Villars P, Calvert LD (1991) Pearson's Handbook of Crystallographic Data for Intermetallic Phases, 2nd edn. Am. Soc. for Metals, Materials Park, OH 44073, and Desk Edition (1997)
24. Parthé E, Gelato L, Chabot B, Penzo M, Cenzual K, Gladyshevskii R (1993) TYPIX-Standardized Data and Crystal Chemical Characterization of Inorganic Structure Types. Gmelin Handbook of Inorganic and Organometallic Chemistry, 8th edn. Springer, Berlin
25. Mishra R, Hermes W, Tegel M, Johrendt W, Pöttgen R (2008) unpublished results
26. Emsley J (1999) The Elements. Oxford University Press, Oxford
27. Donohue J (1974) The structures of the elements. Wiley, New York
28. Zhang K (2007) Xiyou Jinshu Cailiao Yu Gongcheng 36:197
29. Lott BG, Chiotti P (1966) Acta Crystallogr 20:733
30. Stojanovic M, Latturner SE (2007) J Solid State Chem 180:907
31. Gordon RA, Jones CDW, Alexander MG, DiSalvo FJ (1996) Physica B 225:23
32. Nowotny H, Sibert W (1941) Z Metallkd 33:391
33. Haase MG, Schmidt T, Richter CG, Block H, Jeitschko W (2002) J Solid State Chem 168:18
34. Pöttgen R, Borrmann H, Kremer RK (1996) J Magn Magn Mater 152:196
35. Niepmann D, Pöttgen R, Künnen B, Kotzyba G, Rosenhahn C, Mosel BD (1999) Chem Mater 11:1597
36. Kraft R, Pöttgen R, Kaczorowski D (2003) Chem Mater 15:2998
37. Movshovich R, Lawrence JM, Hundley MF, Neumeier J, Thompson JD, Lacerda A, Fisk Z (1996) Phys Rev B 53:5465
38. Pöttgen R, Gulden Th, Simon A (1999) GIT Labor-Fachzeitschrift 43:133
39. Kußmann D, Hoffmann R-D, Pöttgen R (1998) Z Anorg Allg Chem 624:1727
40. Yvon K, Jeitschko W, Parthé E (1977) J Appl Crystallogr 10:73